


ORIGINAL ARTICLE

Novel hKDR mouse model depicts the antiangiogenesis and apoptosis-promoting effects of neutralizing antibodies targeting vascular endothelial growth factor receptor 2

Yuan Cao¹ | Chunyun Sun² | Guitao Huo³ | Huiyu Wang² | Yong Wu¹ | Fei Wang² | Susu Liu¹ | Shijie Zhai¹ | Xiao Zhang² | Haoyang Zhao¹ | Meiling Hu² | Wenda Gu¹ | Yanwei Yang³ | Sanlong Wang³ | Chunnan Liang¹ | Jianjun Lyu¹ | Tiangong Lu⁴ | Youchun Wang⁵ | Liangzhi Xie^{2,6,7} | Changfa Fan¹ 

¹Division of Animal Model Research, National Rodent Laboratory Animal Resources Center, Institute for Laboratory Animal Resources, National Institutes for Food and Drug Control (NIFDC), Beijing, China

²Beijing Engineering Research Center of Protein and Antibody, Sinocelltech Ltd, Beijing, China

³National Center for Safety Evaluation of Drugs, Institute for Food and Drug Safety Evaluation, National Institutes for Food and Drug Control (NIFDC), Beijing, China

⁴School of Life Sciences, Beijing University of Chinese Medicine, Beijing, China

⁵Division of HIV/AIDS and Sexually Transmitted Virus Vaccines, Institute for Biological Product Control, National Institutes for Food and Drug Control (NIFDC), Beijing, China

⁶Beijing Key Laboratory of Monoclonal Antibody Research and Development, Sino Biological Inc., Beijing, China

⁷Cell Culture Engineering Center, Chinese Academy of Medical Sciences and Peking Union Medical College, Beijing, China

Correspondence

Youchun Wang, Division of HIV/AIDS and Sexually Transmitted Virus Vaccines, Institute for Biological Product Control, National Institutes for Food and Drug Control (NIFDC), No. 31 Huatuo Road, Beijing 102629, China.

Email: wangyc@nifdc.org.cn

Liangzhi Xie, Beijing Engineering Research Center of Protein and Antibody, Sinocelltech Ltd., No. 31 Kechuang 7th Street, Beijing, China.

Email: lx@sinocelltech.com

Changfa Fan, Division of Animal Model Research, Institute for Laboratory Animal Resources, NIFDC, No. 31 Huatuo Road, Beijing 102629, China.

Email: fanfc@nifdc.org.cn

Funding information

National Science and Technology Major Project, Grant/Award Number: 2018ZX09101001-004

Abstract

Vascular endothelial growth factor receptor 2 (VEGFR2)/KDR plays a critical role in tumor growth, diffusion, and invasion. The amino acid sequence homology of KDR between mouse and human in the VEGF ligand-binding domain was low, thus the WT mice could not be used to evaluate Abs against human KDR, and the lack of a suitable mouse model hindered both basic research and drug developments. Using the CRISPR/Cas9 technique, we successfully inserted different fragments of the human KDR coding sequence into the chromosomal mouse *Kdr* exon 4 locus to obtain an hKDR humanized mouse that can be used to evaluate the marketed Ab ramucirumab. In addition, the humanized mAb VEGFR-HK19 was developed, and a series of comparative assays with ramucirumab as the benchmark revealed that VEGFR-HK19 has higher affinity and superior antiproliferation activity. Moreover, VEGFR-HK19 selectively inhibited tumor growth in the hKDR mouse model but not in WT mice. The most important binding epitopes of VEGFR2-HK19 are D257, L313, and T315, located in the VEGF binding region. Therefore, the VEGFR2-HK19 Ab inhibits tumor growth by blocking VEGF-induced angiogenesis, inflammation, and promoting apoptosis. To our

Yuan Cao, Chunyun Sun, and Guitao Huo contributed equally to this work and share first authorship.

This is an open access article under the terms of the [Creative Commons Attribution-NonCommercial-NoDerivs](https://creativecommons.org/licenses/by-nc-nd/4.0/) License, which permits use and distribution in any medium, provided the original work is properly cited, the use is non-commercial and no modifications or adaptations are made.

© 2022 The Authors. *Cancer Science* published by John Wiley & Sons Australia, Ltd on behalf of Japanese Cancer Association.

best knowledge, this novel humanized KDR mouse fills the gaps both in an animal model and the suitable in vivo evaluation method for developing antiangiogenesis therapies in the future, and the newly established humanized Ab is expected to be a drug candidate possibly benefitting tumor patients.

KEYWORDS

antiangiogenesis, hKDR humanized mouse, monoclonal antibody, tumor, VEGFR2-HK19

1 | INTRODUCTION

Cancer is a major burden of disease worldwide. Pathological angiogenesis is a hallmark of cancer and various inflammatory and ischemic diseases.¹ A combination of antiangiogenic therapy and immunotherapy is considered the most promising treatment options for cancer.² Among the wide spectrum of endogenous angiogenic molecules, vascular endothelial growth factor (VEGF) is the most studied and has been identified as the most important factor affecting physiological and pathological angiogenesis.³ In addition to placental growth factor, the VEGF family includes VEGF-A, with its predominant isoform VEGF165 and VEGF-B, VEGF-C, and VEGF-D.^{4–6} There are three VEGF receptors, VEGFR1 (Flt-1 in mice), VEGFR2 (Flk-1; KDR), and VEGFR3 (Flt4), which combine with several coreceptors.⁷ Among them, VEGFR2 was confirmed as a viable antitumor therapeutic target, following earlier findings that overexpression of VEGF and VEGFR2 is associated with invasion and metastasis in several malignancies.⁸ Moreover, VEGFR2 is mainly responsible for cell proliferation, vascular permeability, and cell survival through VEGF-induced signaling in endothelial cells,⁹ but the function of VEGFR2 is multifaceted.^{10–13} Consequently, selective VEGFR2 blockade inhibits receptor phosphorylation and tumor angiogenesis, thereby inducing tumor cell apoptosis, ultimately leading to tumor regression.¹⁴

Clinical trials of angiogenesis inhibitors were mainly based on mAbs binding to VEGF/VEGFR, or multitarget receptor tyrosine kinase inhibitors with antiangiogenic specificities.^{15–18} The humanized IgG1 mAb ramucirumab (IMC-1121B), targeting the extracellular domain of VEGFR2 with high affinity, has been approved for the treatment of solid tumors.^{19–22} Preclinical studies confirmed the precise effect and safety,²³ and be widely used as a benchmark human Ab for developing novel Abs for cancer treatment in animal studies.²⁴ The murine version of ramucirumab, DC101, targeting VEGFR2 (Flk-1/KDR), does not cross-react with human VEGFR2, which has been evaluated in C57BL/6 and athymic mice.^{8,25}

Mouse *Kdr* shares 85% nucleotide sequence similarity with human KDR, but they are not functionally equivalent. Knockout of *Kdr* in mice led to death,²⁶ and Hooper et al. found that activation of *Kdr* is critical for hematopoiesis.²⁷ To our best knowledge, no humanized KDR mouse model is available, limiting the in vivo efficacy and safety evaluation of therapeutic products targeting VEGFR. Here a humanized mouse model was established and further functional verification for evaluating therapeutic products was carried out. Moreover, a novel human mAb VEGFR2-HK19 was developed and evaluated.

2 | MATERIALS AND METHODS

2.1 | Cell culture

MC38 cells (Sino Biological Inc.) were cultured in RPMI-1640 medium (Corning) containing 10% FBS. The HUVEC (Lifeline Cell Technology) and VEGFR2 overexpressing 293FT cells (Basic Medical Cell Center) were cultured in phenol red-free M199 medium (Gibco) containing 10% FBS and 5% L-glutamine at 37°C and 5% CO₂.

2.2 | Construction of hKDR humanized mice

A cassette encoding “part of exon 4 to part of exon 7 of human KDR coding sequence (CDS)-part of exon 7 to TAA stop codon of mouse *Kdr* CDS-WPRE-poly-A” was cloned into the corresponding part of exon 4 of mouse *Kdr*. The target sequence of guide RNA (sgRNA) GTTTGAAATCGACCCTCGGCAGG was designed using website <https://zlab.bio/guide-design-resources> and used as a template for in vitro transcription using the MEGA ShortScript T7 High Yield Transcription Kit (Invitrogen). Cas9 mRNA was obtained as described previously.²⁰ Both sgRNA and Cas9 mRNA were purified using the MEGAclean kit (Invitrogen). The targeting vector, sgRNA, and Cas9 mRNA were microinjected into C57BL/6 zygotes subsequently implanted into CD-1 pseudo-pregnant mice.

2.3 | Genotyping

Genomic DNA of the tail from offspring was isolated and subjected to PCR amplification using a two-step PCR strategy. The genomic DNA of hKDR mice yielded amplicons of 2.9 kb and 2.3 kb, respectively. For offspring genotyping, primers F3/R3 were used to identify the hKDR mice with an amplicon of 351 bp (Table 1).

2.4 | Southern blot analysis

Genomic DNA was digested with the restriction enzymes *Bsu36I* (5'-arm) and *NsiI* (3'-arm) and resolved on a 0.8% agarose gel. Upon transfer to a nylon membrane and UV cross-linking, prehybridization and hybridization were carried out at 42°C according to the

TABLE 1 Primer sequences used to identify genetically modified mice

	Primer	Sequence (5'-3')	Product length
Region 1	F1	ATGTAGGGGATGAATAGGATCTC	2.9 kb
	R1	AAATCCTATACCCTACAACGACAAC	
Region 2	F2	CTGGAAGACAGGAACAAATTATCTC	2.3 kb
	R2	CTGACCAGAGAGGACCCTATATC	
	F3	TTTATGTTTCAGGTTTCAGGGGGA	351 bp
	R3	CCAGCACTGTCTAAATCAACGGC	
Southern probe (5')	F5	CTTCGCTGTGCAGGATAATGGTGA	6.2 kb-MT
	R5	GGGAGTAACTTCATCCCCTAGAGACAG	4.2 kb-WT
Southern probe (3')	F5	GTTACCTCGTTTTTCAGTCACTGCATCC	4.3 kb-MT
	R6	AACTGGGGAGAGTAAAGCCTATCTCGC	7.3 kb-WT

Abbreviation: MT, mutant.

instructions for DIG Easy Hyb Granules (Roche). The membrane was then developed using the DIG Detection Kit (Roche), following the manufacturer's instructions. The primers used for probe template synthesis were listed in Table 1.

2.5 | Real-time PCR

Total RNA from hearts, lungs, and kidneys was extracted using TRIzol reagent (Life Technologies) and then converted into cDNA using the RT-PCR kit (Takara) using a Light Cycler 480 Real-Time PCR system. Relative expression levels of hKDR and mKDR were determined using the primers hKDR-F (5'-TGTGGTTCTGAGCCGTCTC-3')/hKDR-R (5'-GTGCTGTTCTTCTTGGTCATCA-3'), and mKDR-F (CAAACCTCAATGTGTCTCTTTGC)/mKDR-R (AGAGTAAAGCCTATCTCGCTGT). Mouse GAPDH mRNA was used as an internal control and quantified using primers GAPDH-F (5'-CAGCAACTCCCCTCTTCCAC-3') and GAPDH-R (5'-TGGTCCAGGGTTTCTTACTC-3'). Each reaction was carried out in triplicate. The data represent the relative transcript abundance of hKDR normalized to GAPDH.

2.6 | Selection of humanized VEGFR2 Ab HK19

The VEGFR2 Abs were screened through phage display from a single-chain variable fragment (scFv) library generated from spleen mRNA of mice immunized with recombinant VEGFR2 protein (Sino Biological Inc.). Specific mAbs against VEGFR2 were screened using recombinant VEGFR2 protein as bait. Candidate scFvs that bind effectively to recombinant VEGFR2 were further developed into chimeric Abs. Chimeric mhK19 showed high affinity and strong inhibitory activity, thus mhK19 was further humanized using the classical complementarity determining region (CDR) transplantation method. IGKV1-NL1*01 and IGHV3-21*01 with 70.5% and 81.6% homology to the heavy and light chains of mhK19, respectively, were selected as humanization templates. The CDRs of humanized templates were then substituted for the corresponding CDRs of mhK19 in light and heavy chain. Finally, a single point mutation P60A was introduced in HCDR2 to obtain humanized Ab VEGFR2-HK19 (IgG1 subtype).

2.7 | Enzyme-linked immunosorbent assay

Human VEGFR2-His protein was coated onto 96-well plates overnight at 4°C, and then blocked with BSA. Either VEGFR2-HK19 or control Ab ramucirumab (2 mg/L) was incubated for 1 h at room temperature (RT). TMB solution was added for color development. Plates were measured at 450 nm (A_{450}) and the data were processed using GraphPad Prism 8.0 software.

To verify whether VEGFR2-HK19 cross-binds to VEGFR2 orthologs from other species, recombinant human, mouse, and rhesus macaque VEGFR2-His proteins were coated onto 96-well plates at concentrations of 0.04, 10, and 10 mg/L, respectively.

2.8 | Flow cytometry and OCTET

Different concentrations of VEGFR2-HK19 were incubated with 3×10^5 293FT-VEGFR2 cells at 4°C for 45 min. After removing the unbound proteins, the cells were incubated with a FITC-labeled secondary Ab for 20 min at 4°C, followed by flow cytometry after washing and filtration. Data analysis was undertaken using FlowJo and GraphPad Prism 8.0 software. The binding kinetics of Abs to VEGFR2 were measured by Octet using an SA sensor (Pall Corporation), after which Abs were added for real-time association and dissociation analysis using Octet96e (ForteBio) at RT.

2.9 | Blocking of VEGFR2/VEGF interaction in vitro

Vascular endothelial growth factor receptor 2-HK19 or ramucirumab was mixed with a fixed amount of VEGFR2-His (1 mg/L), human VEGF-C-His (0.5 mg/L), or human VEGF-D-His (2 mg/L), after which the mixtures were transferred to 96-well plates precoated with VEGF-A (0.5 mg/L) or VEGFR2-Fc (5 mg/L). Samples were incubated for 1 h at RT. The C-His-R023/HRP was used as the secondary Ab for detection. The plates were washed and developed following the procedure described above for ELISA.

2.10 | Blocking of VEGFR2/VEGF interaction in cultured cells

For the competitive 293FT-VEGFR2/VEGF-A blocking assay, different concentrations of VEGFR2-HK19 or ramucirumab were incubated with 3×10^5 293FT-VEGFR2 at 4°C for 20 min. A fixed amount of biotin-labeled VEGF-A (35.7 mg/L) was added to the mixture and incubated at 4°C for 20 min. The cells were incubated with a streptavidin Alexa Fluor 488-labeled secondary Ab for 20 min at 4°C, and the cell binding of VEGF-A was detected by flow cytometry after washing.

2.11 | Neutralization of VEGF-induced HUVEC proliferation

Human umbilical vascular endothelial cells were seeded (4×10^3 cells/well) and incubated with VEGFR2-HK19 or ramucirumab (analog of CYRAMZA, US7498414; Sino Biological), followed by human VEGF-A (10 µg/L), VEGF-C (1000 µg/L), a mixture of human VEGF-C (1000 µg/L)+VEGF-D (8181 µg/L), a mixture of human VEGF-A (25 µg/L)+VEGF-C (1000 µg/L)+VEGF-D (5455 µg/L), mouse VEGF-A (20 µg/L), or mouse VEGF-C (2000 µg/L). In addition,

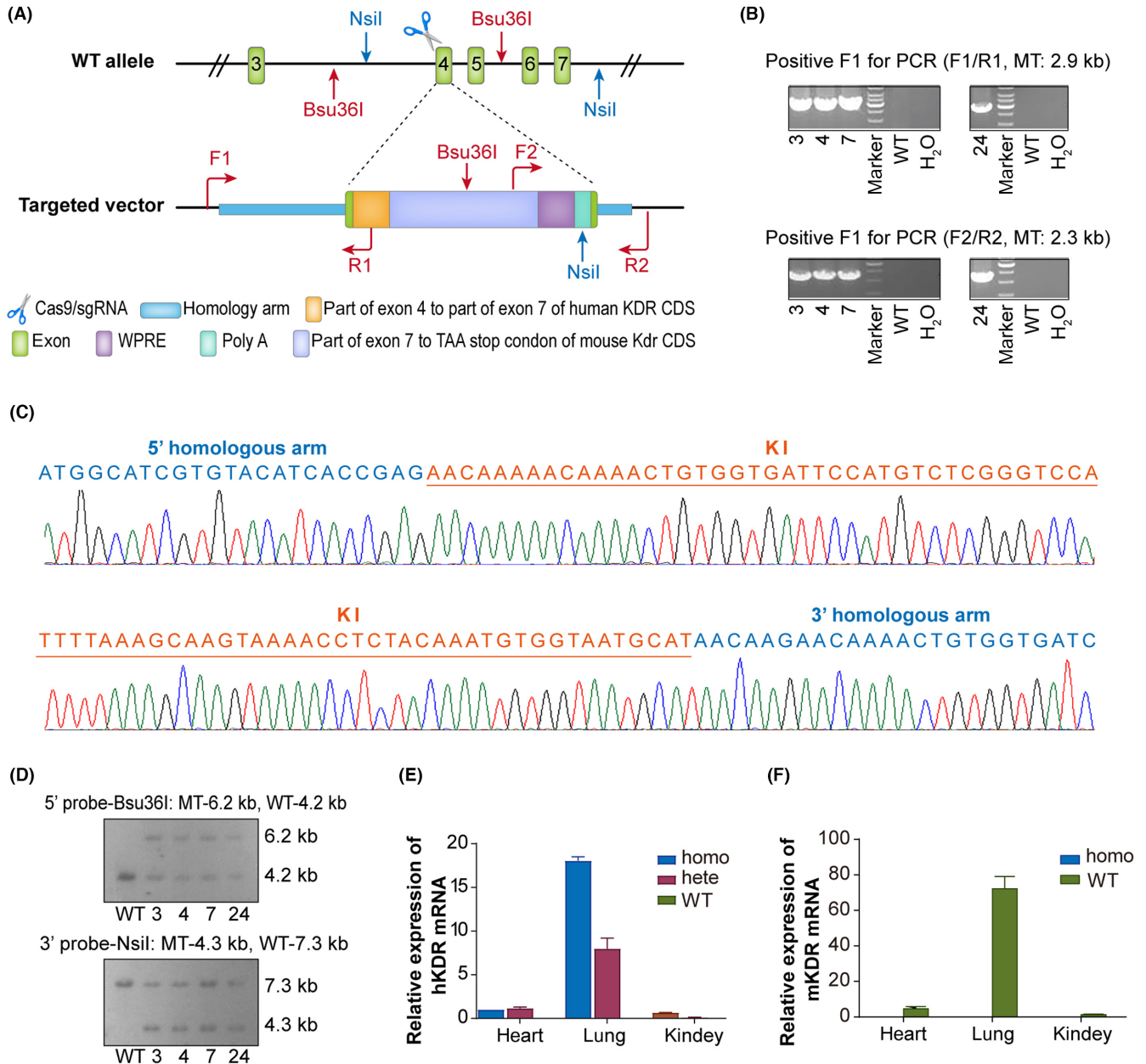


FIGURE 1 Generation of the hKDR humanized mouse model using CRISPR/Cas9 technology. (A) Schematic illustration of targeting. (B) PCR genotyping of F1 hKDR mice. (C) Right insertion was confirmed by sequencing. (D) Insertion was identified by southern blot using 5'- and 3'- probes. Genomic DNA was digested with *Bsu361* and *NsiI*, and produced the expected 6.2 kb and 4.3 kb bands in size, respectively. (E) Detection of hKDR mRNA expression in heart, lung, and kidney tissues ($n = 3$). (F) mKDR mRNA expression was detected in heart, lung, and kidney tissues ($n = 3$). Values are presented as means \pm SD of three mice and were normalized to GAPDH levels. CDS, coding sequence; hete, heterozygous; homo, homozygous; KI, knock in; MT, mutant; WT, wild-type

a blank well, M group (without Ab, but with VEGFs), and M' group (without Ab and VEGFs) were also included. Plates were incubated for 72h at 37°C, followed by the addition of WST-8 (GLT008; Nanjing Robiot Co., Ltd), then plates were measured at 450nm and 630nm using a microplate reader (SpectraMax i3x; Thermo Fisher). The neutralization rate was then calculated using the formula: neutralization rate (%) = $(M - \text{antibody}) / (M - M') \times 100\%$.

2.12 | Homology modeling and molecular docking

The Antibody Model program in DS 4.0 (Accelrys Software Inc.), was used to model VEGFR2-HK19 and the VEGFR2 structure was extracted from the PDB database (ID: 3V2A). The VEGFR2-HK19 model and VEGFR2 structure were docked using the ZDOCK program. According to the docking results, the top 10 candidates were optimized using RDOCK, after which the optimal model was further analyzed using the Protein Interface Analysis program.

2.13 | Tumor study in hKDR humanized mice in vivo

MC38 cells (5×10^6 cells per mice) were subcutaneously inoculated into the dorsal flank of 3-week-old hKDR and C57BL/6 mice for the tumor bearing model. The tumor size was measured using a slide caliper and calculated as $\text{length} \times \text{width}^2 \times 0.5$. When the tumor size reached 100–200mm³, the mice were randomly divided into different

groups ($n = 8$ per group) and treated with ramucirumab (20mg/kg i.v.), VEGFR2-HK19 (20mg/kg i.p.), DC101 (20mg/kg i.p.), or solvent twice weekly for 3 weeks. Bodyweights were determined during the experiment. At the end of the experiment, blood samples were collected from the abdominal aorta of anesthetized mice. Cytokines in sera were tested using a Bio-Plex 200 system and Bio-Plex Pro Mouse Cytokine 23-plex Assay (M60009RDPD; Bio-Rad). Tumor tissues were collected, weighed, and frozen at -80°C for further analysis.

2.14 | Western blot analysis

Tissues were homogenized in RIPA lysis buffer supplemented with a 1× proteinase inhibitor cocktail (Roche). Samples were separated on 8% polyacrylamide SDS-PAGE gels, then transferred onto a methanol-activated PVDF membrane. Mouse or rabbit mAbs against p-VEGFR2, VEGFR2, cleaved caspase-9, procaspase-9, and GAPDH (1:1000 dilution; Cell Signaling Technology) were added, followed by HRP-conjugated anti-mouse IgG or anti-rabbit IgG (1:10,000, Santa Cruz Biotechnology). The Immobilon Western Chemiluminescent HRP Substrate kit (Millipore) was used to develop the protein bands.

2.15 | Histopathology and immunohistochemistry

Tumor tissues were fixed in 10% neutral-buffered formalin, H&E staining was carried out on 5 μm paraffin sections. For immunohistochemistry,

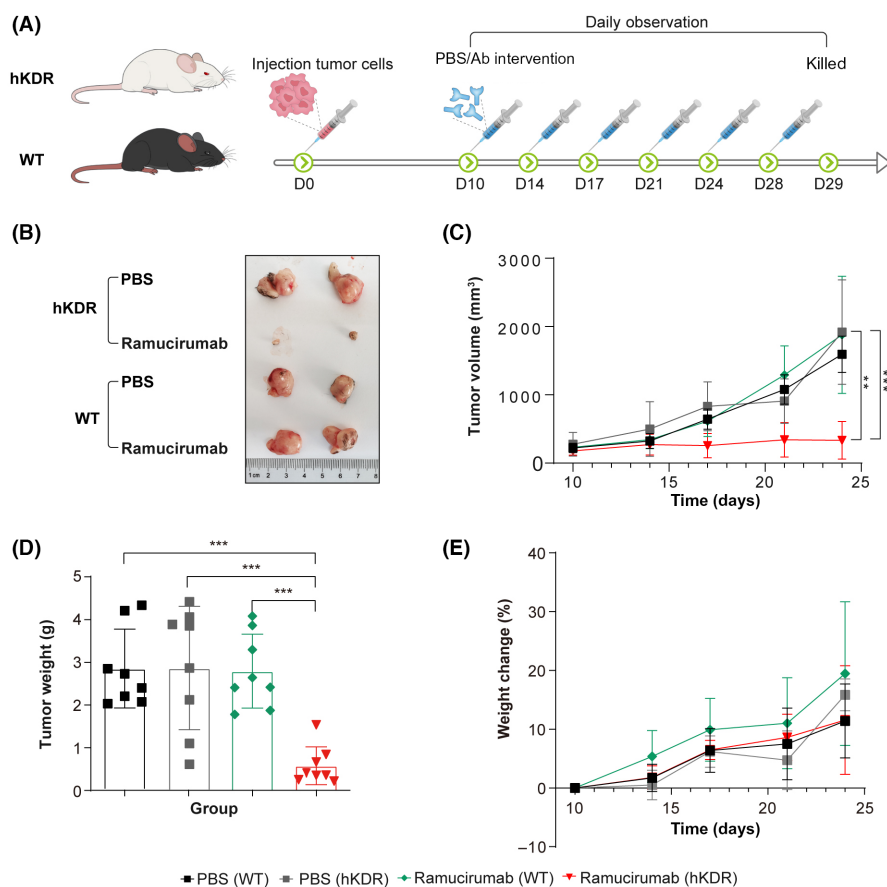


FIGURE 2 Humanized vascular endothelial growth factor receptor 2 (VEGFR2) Ab selectively inhibited tumor growth in hKDR mice. (A) Mice bearing MC38-derived xenograft tumors were treated with ramucirumab. (B) Tumors from different treatment groups. (C) Tumor growth in different groups. (D) Tumor weight was measured at the end of the experiment. (E) Bodyweight change was measured at various time points. Group 1, PBS (WT mice); group 2, PBS (hKDR mice); group 3, ramucirumab (WT mice); group 4, ramucirumab (hKDR mice). All data represent the mean of 8 mice per group. Error bars, SD. * $p < 0.05$, ** $p < 0.01$, *** $p < 0.001$

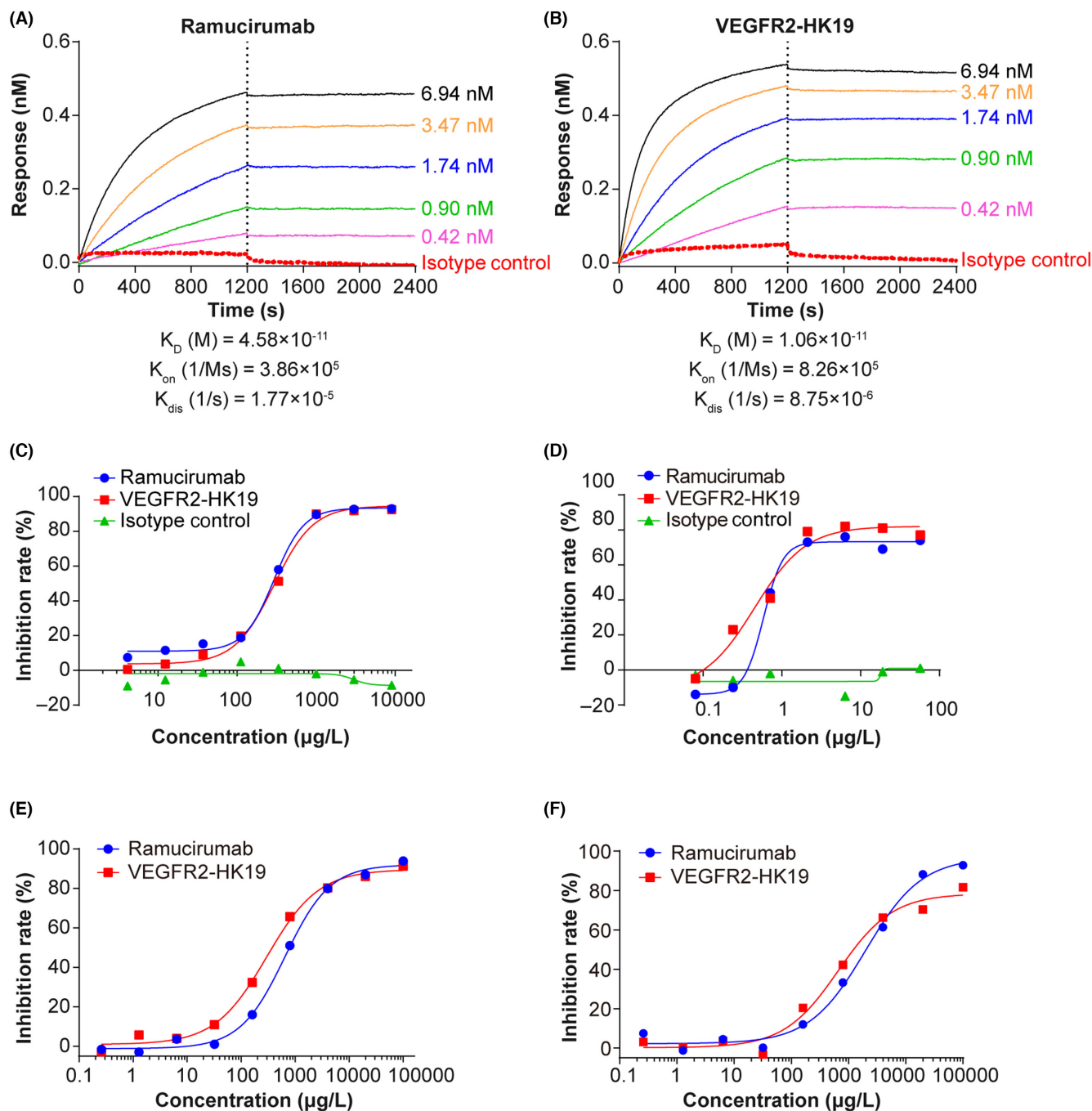


FIGURE 3 Characteristics of the newly established vascular endothelial growth factor receptor 2 (VEGFR2)-HK19 humanized Ab. (A,B) Octet affinity analysis of (A) ramucirumab and (B) VEGFR2-HK19 with recombinant VEGFR2 protein. (C,D) VEGFR2-HK19 blocked the binding of human VEGF-A to (C) recombinant VEGFR2 protein and (D) VEGFR2-overexpressing 293FT cells according to ELISA and FACS analysis, respectively. (E,F) VEGFR2-HK19 inhibited the proliferation of HUVECs induced by (E) human VEGF-A or (F) human VEGF-A + VEGF-C + VEGF-D

CD31 and CD34 (1:100 dilution; HuaAn Biotechnology Co., Ltd) staining was carried out. The apoptotic cells in the tumor tissue were detected by TUNEL assay using an apoptotic cell detection kit (Merck Millipore). Images were taken with a Panoramic MIDI (3DHISTECH) microscope. Microvessel density was calculated using Image Pro Plus 6 software in 12 randomly selected fields at 200 \times and 400 \times magnifications.

2.16 | Statistical analysis

Data are presented as mean \pm SD and analyzed using GraphPad Prism 8.0. Student's *t*-test or one-way ANOVA was used to assess the statistical significance of differences between the groups. $p < 0.05$ was considered to indicate statistical significance.

3 | RESULTS

3.1 | Generation of hKDR humanized mouse model using CRISPR/Cas9 technology

An insert spanning part of exon 4 to part of exon 7 of human *KDR* CDS, and part of exon 7 to the TAA stop codon of mouse *Kdr* CDS was inserted into the mouse *Kdr* exon 4 locus, followed by a woodchuck hepatitis virus posttranscriptional regulatory element (WPRE) and poly-A sequence. This design resulted in an intrinsic expression profile of hKDR under control of mouse *Kdr* promoter (Figure 1A). The targeting vector and sgRNA and Cas9 mRNA were injected into the zygotes of C57BL/6 mice, resulting in two positive insertions in 93 offspring. The surviving founder was crossed with C57BL/6 mice and generated a successful germline transmission. F1 positive mice were confirmed by PCR genotyping (Figure 1B), sequencing (Figure 1C), and southern blotting (Figure 1D). The homozygous mice were designated as C57BL/6-*Kdr*^{em1(hKDR)}/NIFDC, abbreviated as hKDR mice. The mRNA expression of hKDR was detected in heart, lung, and kidney tissues of hKDR mice (Figure 1E), but not in WT mice. No mRNA expression of mKDR was detected in homozygous hKDR mice (Figure 1F), indicating mKDR was replaced fully by hKDR.

3.2 | Ramucirumab selectively inhibited tumor growth in hKDR mice

To verify the suitability of the hKDR mouse model for the evaluation of drugs targeting VEGFR in vivo, a tumor-bearing model was established by subcutaneous injection of MC38 cells.²⁴ Both hKDR and WT mice bearing tumors were treated with human ramucirumab or PBS (Figure 2A). The results showed that the tumor shape (Figure 2B), tumor volume (Figure 2C), and weight (Figure 2D) decreased in hKDR mice after treatment with ramucirumab, compared with the PBS control group ($p < 0.01$). By contrast, ramucirumab treatment did not reduce tumor volume, or weight in WT mice, which was similar to the PBS group ($p > 0.05$). The bodyweight change corresponded well with tumor growth (Figure 2E). These results indicated that the human mAb only inhibited tumor growth in hKDR mice but not in WT mice; only the hKDR mice were fit for evaluation of the in vivo effect of ramucirumab.

3.3 | Generation and evaluation of neutralizing Ab VEGFR2-HK19

An unmet clinical need has compelled us to develop a new Ab targeting VEGFR2 using phage display platforms and high-throughput screening strategies.²⁸ Candidate scFvs that bind effectively to recombinant VEGFR2 were further developed into human-mouse chimeric Abs. One chimeric Ab, named mhK19, showed highest affinity and a strong inhibitory effect on VEGF-induced endothelial cell proliferation. Therefore, it was further humanized and named VEGFR2-HK19.

TABLE 2 Vascular endothelial growth factor receptor 2 (VEGFR2)-HK19 blocked the induction of endothelial cell proliferation by vascular endothelial growth factor (VEGF)

Stimulant	Antibody	EC ₅₀ (μg/L)	Max (%)
VEGF-A	Ramucirumab	649.8	93.9
	VEGFR2-HK19	296.4	91.3
VEGF-A+VEGF-C+VEGF-D	Ramucirumab	1986	93
	VEGFR2-HK19	663.2	82
VEGF-C	Ramucirumab	87.45	100.7
	VEGFR2-HK19	23.85	100.3
VEGF-C+VEGF-D	Ramucirumab	86.02	95.3
	VEGFR2-HK19	42.65	98.9

The EC₅₀ of VEGFR2-HK19 binding to recombinant VEGFR2-His protein and VEGFR2-overexpressing 293FT cells was 191.5 and 17.18 μg/L, respectively (Figure S1A,B). The K_D value of VEGFR2-HK19 combined with recombinant human VEGFR2 protein was 1.06 × 10⁻¹¹ M, while that of ramucirumab was 4.58 × 10⁻¹¹ M (Figure 3A,B). These results show that VEGFR2-HK19 possesses high binding specificity for the VEGFR2 antigen, better than ramucirumab.

Next, the ability of VEGFR2-HK19 to inhibit the binding of human VEGFs to VEGFR2 was investigated using competitive binding assays with both purified proteins in vitro and cultured cells. Combined VEGFR2-HK19 and ramucirumab prevented human VEGF-A from binding to either VEGFR2 protein or 293FT cells overexpressing VEGFR2 (Figure 3C,D). Moreover, both Abs also prevented the binding of other subtypes of human VEGF, including VEGF-C and -D (Figure S1C,D). In addition, the EC₅₀ of VEGFR2-HK19 was comparable to that of ramucirumab or even slightly lower (Table S1), indicating that both VEGFR2-HK19 and ramucirumab have high ligand competitiveness.

The activity of VEGFR2-HK19 inhibiting angiogenesis was tested. The results show that VEGFR2-HK19 neutralized endothelial cell proliferation induced by a single human VEGF isoform and showed high neutralization ability with different human VEGF mixtures (Figures 3E,F and S1E,F), the EC₅₀ and maximum inhibition rates with different VEGFs are shown in Table 2. As expected, the relatively low EC₅₀ of VEGFR2-HK19 suggests that it could have superior antiproliferation activity compared to ramucirumab.

3.4 | Ramucirumab and VEGFR2-HK19 share most binding epitopes

The epitopes bound by VEGF-A are located in the second and third domains of VEGFR2.²⁹ Homology modeling and molecular docking predicted that the key binding peptides of VEGFR2-HK19 were ¹³⁷YITENK¹⁴² and ¹⁶⁴RYPEKR¹⁶⁹ from domain 2, as well as ²⁵⁵GIDFNWEY²⁶² and ³¹⁰SSGLMTKK³¹⁷ from domain 3. To further verify these key epitopes, various VEGFR2 variants were generated and assayed for their ability to bind VEGFR2-HK19, ramucirumab, or

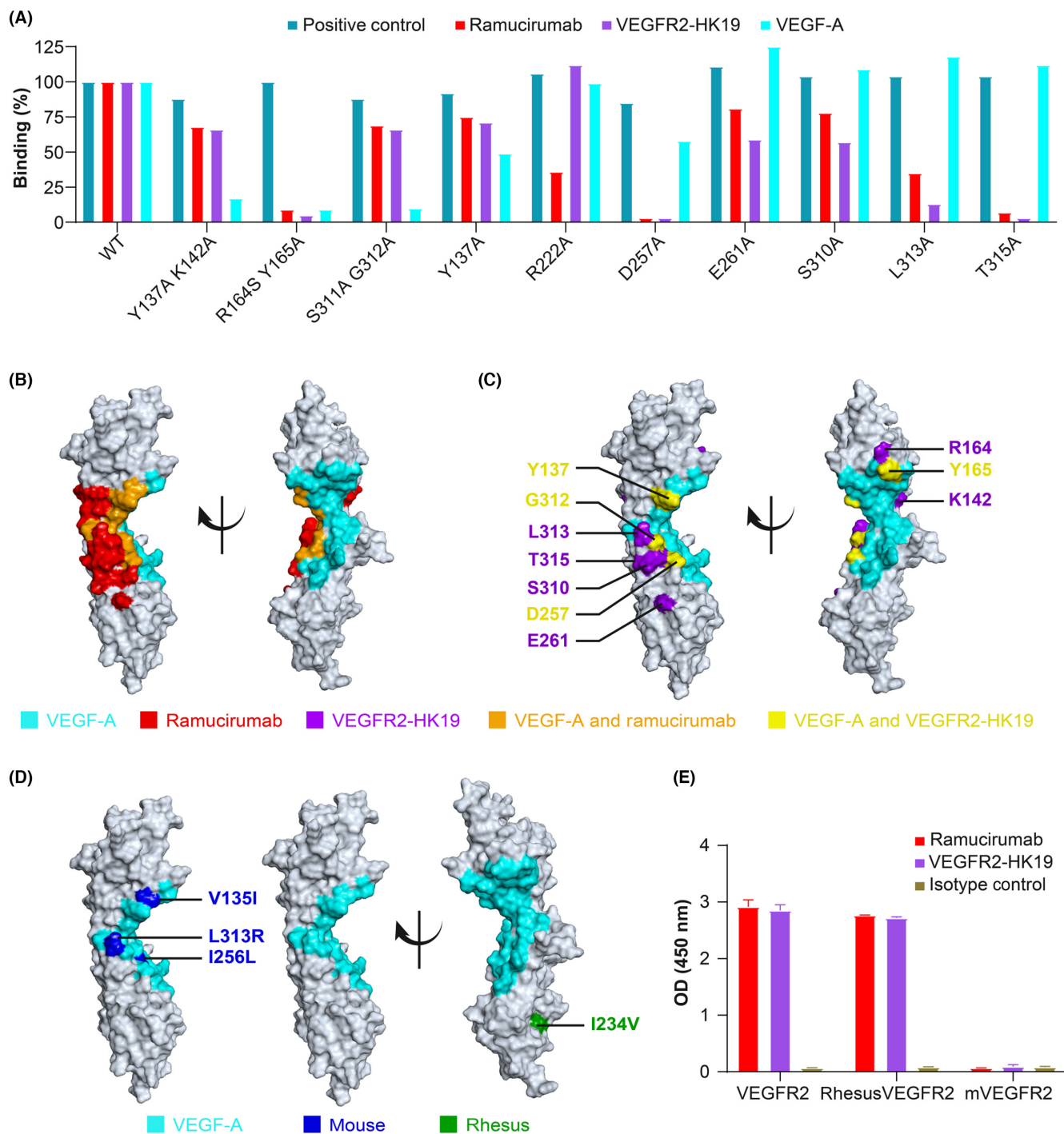


FIGURE 4 Epitope mapping and cross-binding of vascular endothelial growth factor receptor 2 (VEGFR2)-HK19 to VEGFR2. (A) Epitopes were analyzed by ELISA using recombinant VEGFR2 variants. (B) Human VEGF-A and ramucirumab epitopes are displayed based on the crystal structure of human VEGF-A/VEGFR2 in the PDB database (3V2A) or the ramucirumab/VEGFR2 crystal structure (3S37). Cyan, epitopes of human VEGF-A; red, ramucirumab; dark yellow, overlapping epitopes. (C) Based on the detection results of (A), VEGFR2-HK19 epitopes were labeled on the crystal structure of VEGFR2 (PDB 3S37). Cyan, human VEGF-A epitopes; purple, VEGFR2-HK19 epitopes; light yellow, overlapping epitopes. (D) Different sites in human VEGF-A ligand-binding regions of VEGFR2 from different species. Blue, differences between humans and mice; green, differences between humans and rhesus macaques. (E) VEGFR2-HK19 and ramucirumab do not cross-bind with mouse VEGFR2 in ELISA.

VEGF-A. The key epitopes of VEGF-A and ramucirumab (Figure 4A,B) are consistent with previous results of crystal structure analysis.^{30,31} The most important binding epitopes of VEGFR2-HK19 are R164/Y165, D257, L313, and T315, while other sites such as Y137/K142,

S311/G312, Y137, E261, and S310 are also essential (Figure 4A). In addition, Y137/K142, R164/Y165, S311/G312, Y137, and D257 were identified as the key epitopes that simultaneously affected the binding of VEGFR2-HK19 and VEGF-A to VEGFR2, showing

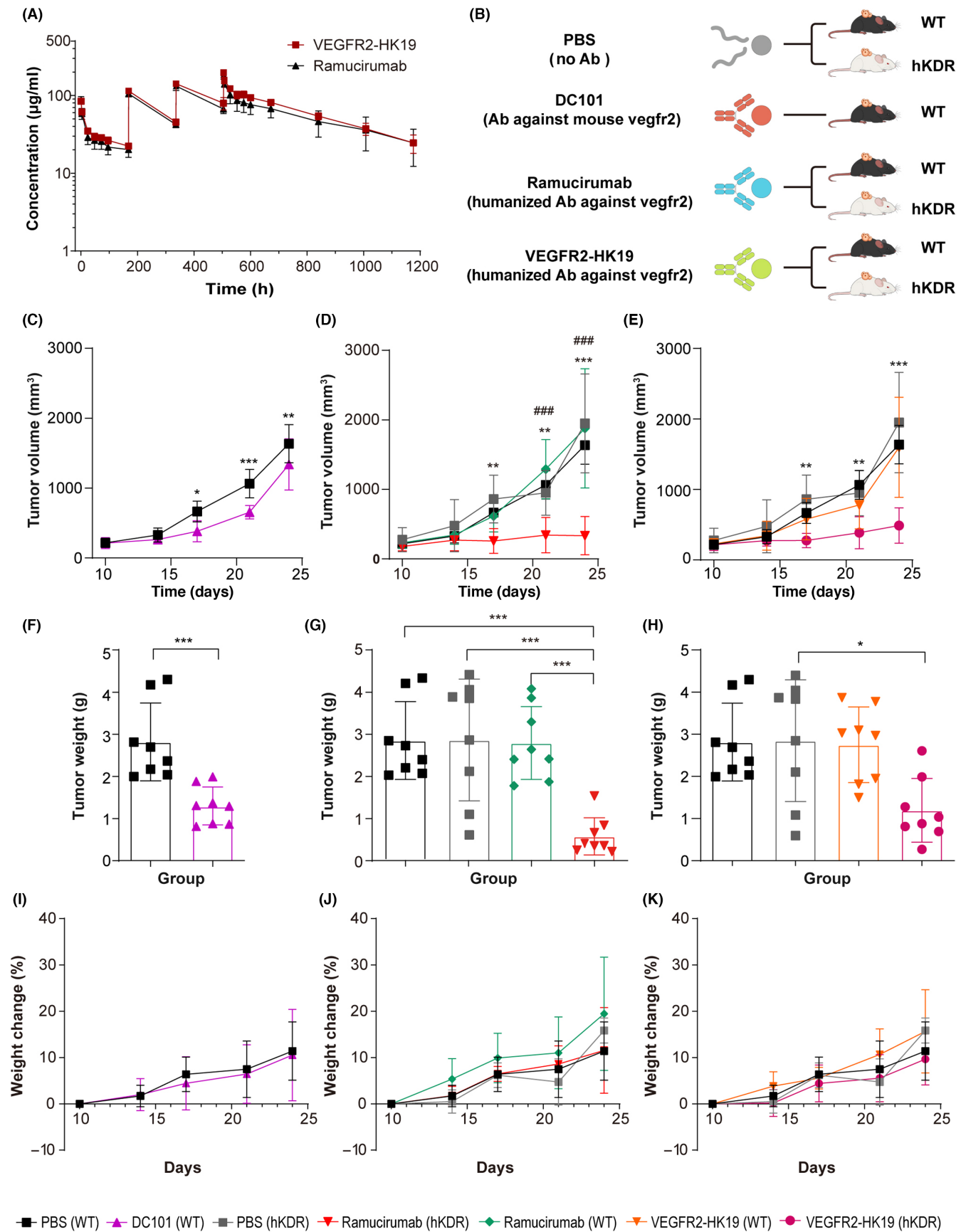


FIGURE 5 Therapeutic efficacy of vascular endothelial growth factor receptor 2 (VEGFR2)-HK19 in mice. (A) Time profile of the VEGFR2-HK19 and ramucirumab serum concentration following intravenous administration ($n = 6$). (B) Treatment schedules. (C-E) Tumor growth ($n = 8$) (F-H) and tumor weight at the end of the treatment ($n = 8$). (I-K) Bodyweight change ($n = 8$). All data are shown as means \pm SD. * $p < 0.05$, ** $p < 0.01$, *** $p < 0.001$

that the VEGFR2-HK19 Ab and VEGF-A had overlapping epitopes (Figure 4A,C). These results revealed that VEGFR2-HK19 shares most binding epitopes with ramucirumab, such as R164/Y165, D257, L313, and T315, confirming that their antiangiogenic effect is through direct inhibition of ligand-binding. The sites R222, E261, S310, and L313 had different effects on the binding affinity of the two mAbs.

3.5 | Cross-binding of VEGFR2-HK19 to receptor orthologs

The VEGF-A ligand-binding regions in VEGFR2 have three different amino acid residues between humans and mice, namely L313R, I256L, and V135I, and no difference between humans and rhesus macaques (Figure 4D). L313 is the core epitope of VEGFR2-HK19, while I256 is adjacent to the core epitope D257, which could affect the binding of humanized Abs to mouse VEGFR2. The ELISA results further confirmed that VEGFR2-HK19 and ramucirumab did not cross-bind to mouse VEGFR2 but retained binding capacities for rhesus macaque VEGFR2 (Figure 4E). The differences in VEGFR2 between human and mice could explain why humanized KDR mice were suitable for the evaluation of in vivo antitumor activities, but WT mice were not (Figure 2).

3.6 | Strong antitumor effect of VEGFR2-HK19 in hKDR mice

To investigate the in vivo pharmacokinetics, 5 mg/kg VEGFR2-HK19 or ramucirumab was given to CD-1 mice intravenously with multiple doses. Notably, VEGFR2-HK19 showed a long half-life of up to 295.3 (295.3 ± 64.75) h, indicating that the stable serum level of VEGFR2-HK19 could maintain its effect in vivo (Figure 5A).

As mouse VEGF-A and VEGF-C cross-activate human VEGFR2 receptor and VEGFR2-HK19 and ramucirumab cross-inhibit mouse VEGF-induced human HUVEC cell growth (Figure S3), humanized hKDR mice can be used to evaluate VEGFR2 Ab activity in vivo. The murine version of ramucirumab, DC101, together with the two humanized Abs were included to test the antitumor activities (Figure 5B). On day 17, the DC101 Ab began to show antitumor activity, and the tumor volumes decreased compared with the PBS group in wild-type mice (Figure 5C). After dissection, the tumor weight was significantly lower than the PBS control group (Figure 5F). Serum tumor necrosis factor- α (TNF- α) level decreased slightly ($p > 0.05$; Figure S2). Ramucirumab showed no antitumor activity in WT mice, but it had obvious antitumor activity in hKDR mice (Figure 5D,G), accompanied by a decline of blood TNF- α (Figure S3).

Similarly, VEGFR-HK19 decreased the tumor size and weight in hKDR mice but not in WT mice (Figure 5E,H). Mouse body weight change was monitored, as shown in Figure 5I-K, and no adverse effects were noted. Overall, VEGFR2-HK19 had a strong antitumor effect in hKDR mice, and showed a promising therapeutic efficacy in vivo. Based on the tumor volume (Figure 5D,E) and tumor weight (Figure 5G,H), VEGFR2-HK19 had similar in vivo antitumor activity to that of ramucirumab.

3.7 | VEGFR2-HK19 inhibits tumor angiogenesis by promoting apoptosis

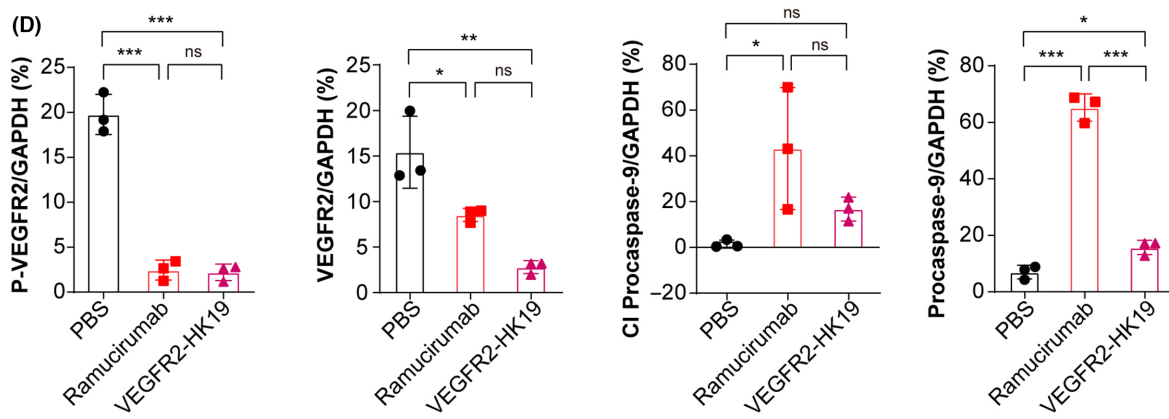
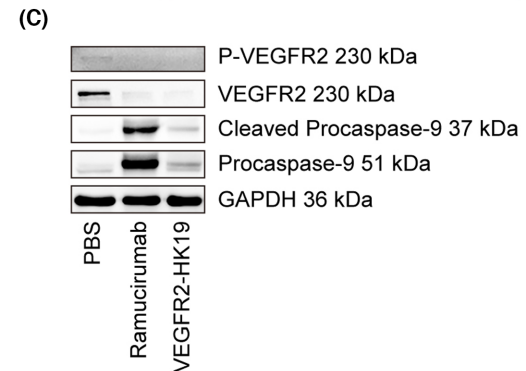
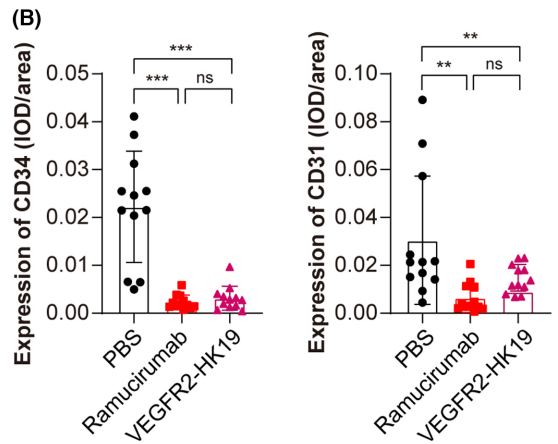
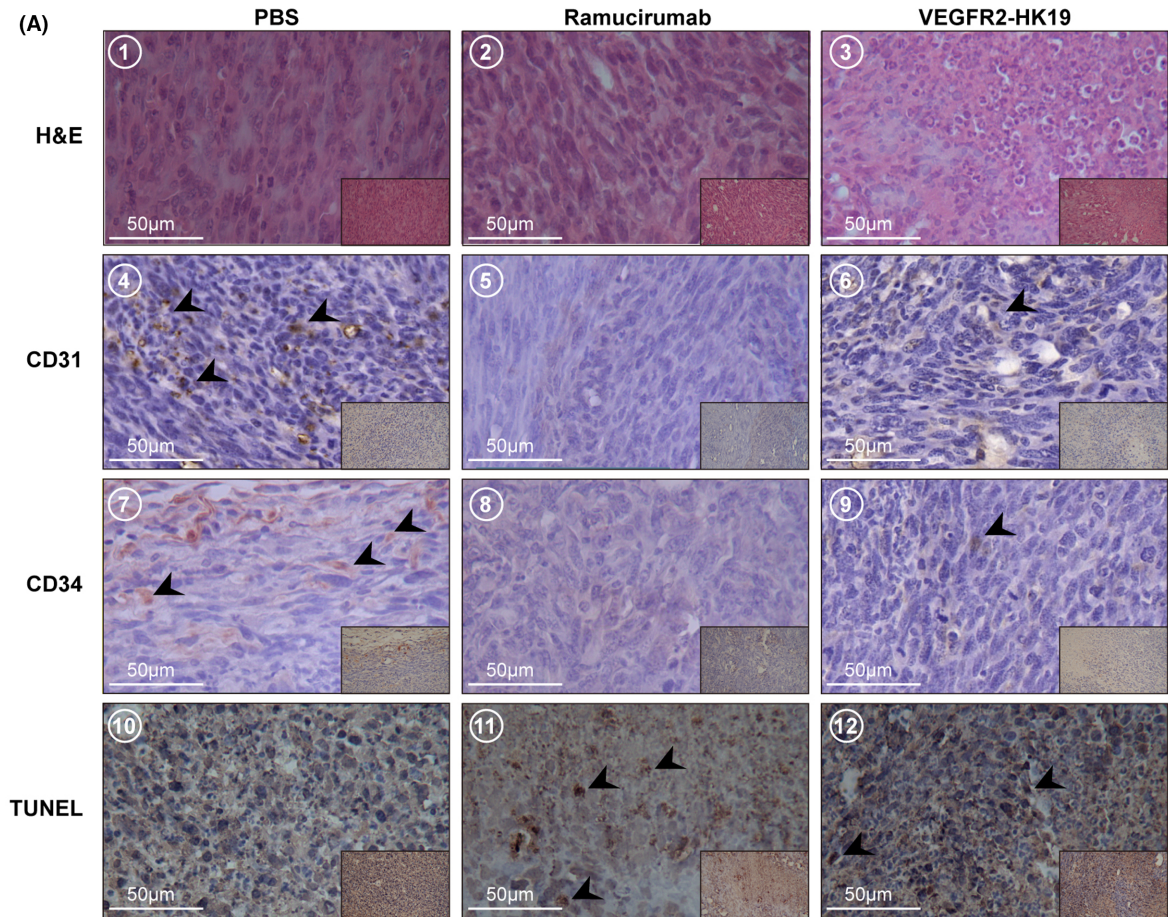
CD31 is a widely used endothelial marker for quantifying angiogenesis by calculating microvessel density (MVD).³² CD34 is the most sensitive marker of neovascular endothelial cells and can reflect the proliferation level of tumor cells to a certain extent.³³ Here we observed that cells from tumor tissues in the PBS group were disordered, and the nuclei were irregularly distributed. Gaps in the cytoplasm might suggest tumor microvessel rupture. By contrast, the arrangement of tumor cells in the VEGFR2-HK19 and ramucirumab groups was normalized, and MVD obviously decreased compared with the PBS group (Figure 6A,B), which was correlated with reduced expression of endothelial cell markers CD31 and CD34 according to immunohistochemical staining.

Similarly, TUNEL staining in the PBS group showed few apoptotic cells and the normal cell nucleus are blue, while in ramucirumab and VEGFR2-HK19 treated groups, the cells were arranged irregularly and were brown and shrunken (Figure 6A). Western blot analysis (Figure 6C) revealed that VEGFR2-HK19 significantly reduced phosphorylated and total VEGFR2 (Figure 6D). The increased procaspase-9 expression caused by Ab treatments supported their effective roles in apoptosis (Figure 6D). Together, these data suggested that VEGFR2-HK19 inhibits tumor growth by promoting apoptosis and decreasing vessel density, similar to a previous report,⁸ and was as effective as ramucirumab.

4 | DISCUSSION

Antiangiogenesis is considered a promising antitumor strategy,³⁴⁻³⁶ and several antitumor inhibitors, including ramucirumab, have been developed to disrupt the signaling pathways of VEGFs.²¹ Due to the lack of suitable animal models, the in vivo efficacy of therapeutic products was evaluated mostly in nonhumanized mice, and in a few cases, in nonhuman primates.^{12,37-39} Nevertheless, wild mouse VEGFR is not a functional substitute of human's, implying WT mice

FIGURE 6 Vascular endothelial growth factor receptor 2 (VEGFR2)-HK19 inhibited angiogenesis and induced apoptosis. (A) H&E and immunohistochemical staining with Abs against CD31 and CD34, and TUNEL staining results in mouse tumor tissue sections. Arrows indicate CD31⁺ and CD34⁺ cells and apoptotic cells. (B) Effects of VEGFR2-HK19 on microvessel density in tumor tissues ($n = 12$). (C,D) Western blot analysis of p-VEGFR2, VEGFR2, cleaved caspase-9, and procaspase-9 protein levels in tumor tissues ($n = 3$). All data are shown as means ± SD. * $p < 0.05$, ** $p < 0.01$, *** $p < 0.001$. ns, no significance



are not an appropriate evaluation animal model. Therefore, a genetically stable humanized KDR mouse model is quite necessary. Multiple *in vivo* validation experiments (Figures 2 and 3) showed that this hKDR humanized mouse could effectively evaluate the therapeutic efficacy of Abs, which is highly desirable for basic research and drug development, especially now, when nonhuman primates are very, very scarce.

The key binding sites for the investigated Abs are residues 135, 313, and 256 of VEGFR. Human, nonhuman primate, and mouse VEGFR orthologs have different amino acids at these sites: valine, leucine, and isoleucine for human and nonhuman primate orthologs mice, and isoleucine, arginine, and leucine for mice, respectively (Figure 4D). This difference could be the reason why the Abs against human VEGFR fail to bind to its mouse ortholog. The cross-binding experiments also showed that ramucirumab and VEGFR2-HK19 had a good binding for VEGFR2 from humans and nonhuman primates but a weak affinity for the murine receptor (Figure 4E). To our best knowledge, this novel hKDR mouse could be the first humanized model.

So far, hundreds of thousands of patients have benefited from drugs targeting the angiogenic protein VEGF.⁴⁰ Various inhibitors, such as small molecules and mAbs targeting the VEGF/VEGFR2 pathway, have revolutionized oncological treatment.^{15–18} In light of the potential need, the humanized mAb VEGFR2-HK19 was developed and characterized in detail. The VEGFR2-HK19 mAb has a long *in vivo* half-life, which was comparable to that of ramucirumab.²³ It has also a higher affinity, stronger neutralization activity (Figures 3E,F and S1E,F), and similar *in vivo* antitumor potential (Figure 5). Ramucirumab and VEGFR2-HK19 share five key binding sites, including R164, Y165, D257, L313, and T315, implying the two have similar functions.

Ramucirumab and VEGFR2-HK19 effectively inhibited the tumor growth in humanized hKDR mice, except in WT mice (Figure 5). The decreased microvessel density and decreased protein expression of VEGF2 in the tumors from treated hKDR mice might be due to the Abs binding to human VEGFR2, which could affect the overall tumor microenvironment to restrict tumor growth.

It has been reported that DC101 treatment and subsequent tumor cell apoptosis reduce vascular density, leading to slower tumor cell proliferation in a mouse model.⁸ Therefore, we speculated that VEGFR2-HK19 has such a similar effect. Apoptosis is a cellular suicide program critical for development and tissue homeostasis.⁴¹ Excess apoptosis is associated with degenerative disorders,⁴² while a failure of apoptosis contributes to tumor development and progression.⁴³ Caspase-9 is a key molecule that responds to various apoptotic signals to activate the intrinsic or mitochondrial pathway. Failing to activate caspase-9 has profound physiological and pathophysiological effects, leading to degenerative and developmental disorders and cancer.^{41,44} In this study, we observed that VEGFR2-HK19 blocks the induction of HUVEC proliferation by VEGF. Treatment with VEGFR2-HK19 increased the levels of cleaved caspase-9 and procaspase-9 in xenografted tumors implanted into hKDR mice, and TUNEL staining indicated that VEGFR2-HK19 promoted apoptosis in hKDR mice. It was reported that the phosphorylation of VEGFR2 in endometrial

cancer cells is associated with a significantly poorer prognosis.⁴⁵ In our research, the expressions of p-VEGFR2 and VEGFR2 in the tumors of VEGFR2-HK19-treated hKDR mice decreased, compared with PBS treatment, implying that VEGFR2-HK19 can inhibit tumor angiogenesis, thus achieving an antitumor effect that indicated that VEGFR2-HK19 inhibited tumor growth by inducing apoptosis.

Yoh et al. reported that ramucirumab plus docetaxel safely prolonged the survival of patients with non-small-cell lung cancer in a phase II study.⁴⁶ The results in this study indicated that the antitumor mechanism of VEGFR2-HK19 might not be the same as that of ramucirumab. The protein levels of cleaved caspase-9 and procaspase-9 in the tumors of ramucirumab treated hKDR mice were higher than in the VEGFR2-HK19 treated group, which was consistent with the TUNEL results (Figure 6). We, therefore, thought that ramucirumab mainly acts by inducing apoptosis to inhibit tumor growth, while the proapoptotic effect of VEGFR2-HK19 is weaker than that of ramucirumab; however, the two have similar *in vivo* antitumor activity (Figure 5).

We established the first humanized KDR mouse model and analyzed the key differential amino acids in the VEGFR binding domains of humans and mice. A new mAb targeting human VEGFR was developed and evaluated *in vitro* and *in vivo*, revealing its potential as a clinical drug candidate (Figure S4).

AUTHOR CONTRIBUTIONS

CF, LX, and YW designed the studies, YC, GH, YW, SL, SZ, HZ, WG, YY, SW, CL, JL, and TL performed the animal experiments, pathological analysis, and data collections. CS, HW, FW, XZ, and MH performed the antibody experiments. CY, HW, CF, CS, and TL contributed to manuscript preparation. CF, LX, and YW revised the manuscript.

ACKNOWLEDGMENTS

We thank Ms. Chunming Sun for drawing the graphics.

FUNDING INFORMATION

This work was supported by a National Science and Technology Major Project (2018ZX09101001-004).

DISCLOSURE

The authors have declared that no competing interest exists. The raw data supporting the conclusions of this article will be made available by the authors, without undue reservation.

ETHICS STATEMENT

The research protocol was approved by an institutional review board (#2021-B-002).

ANIMAL STUDIES

Experiments involving animals were approved by the Ethics Committee of National Institutes for Food and Drug Control (NIFDC) and performed in accordance with Institutional Animal Care and Use Committee of NIFDC guidelines (#2021-B-002).

ORCID

Changfa Fan  <https://orcid.org/0000-0001-5556-2025>

REFERENCES

- Carmeliet P, Jain RK. Angiogenesis in cancer and other diseases. *Nature*. 2000;407:249-257. doi:10.1038/35025220
- Song YX, Fu Y, Xie Q, Zhu WJ, Zhang BC. Anti-angiogenic agents in combination with immune checkpoint inhibitors: a promising strategy for cancer treatment. *Front Immunol*. 2020;11:1956-1972. doi:10.3389/fimmu.2020.01956
- Carmeliet P. Angiogenesis in life, disease and medicine. *Nature*. 2005;438:932-936. doi:10.1038/nature04478
- Chloe P, Viviane M, Maria A, et al. Molecular pharmacology of VEGF-A isoforms: binding and signalling at VEGFR2. *Int J Mol Sci*. 2018;19:1264-1651. doi:10.3390/ijms19041264
- Fearnley GW, Odell AF, Latham AM, et al. VEGF-A isoforms differentially regulate ATF-2-dependent VCAM-1 gene expression and endothelial-leukocyte interactions. *Mol Biol Cell*. 2014;25:2509-2521. doi:10.1091/mbc.E14-05-0962
- Ferrara N. Vascular endothelial growth factor: basic science and clinical progress. *Endocr Rev*. 2004;25:581-611. doi:10.1210/er.2003-0027
- Olsson AK, Dimberg A, Kreuger J, Claesson-Welsh L. VEGF receptor signaling—in control of vascular function. *Nat Rev Mol Cell Biol*. 2006;7:359-371. doi:10.1038/nrm1911
- Prewett M, Huber J, Li Y, et al. Antivascular endothelial growth factor receptor (fetal liver kinase 1) monoclonal antibody inhibits tumor angiogenesis and growth of several mouse and human tumors. *Cancer Res*. 1999;59:5209-5218.
- Yu Y, Cai W, Pei C, Shao Y. Rhamnazine, a novel inhibitor of VEGFR2 signaling with potent anti-angiogenic activity and anti-tumor efficacy. *Biochem Biophys Res Commun*. 2015;458:913-919. doi:10.1016/j.bbrc.2015.02.059
- Spannuth WA, Nick AM, Jennings NB, et al. Functional significance of VEGFR-2 on ovarian cancer cells. *Int J Cancer*. 2009;124:1045-1053. doi:10.1002/ijc.24028
- Donnem T, Al-Saad S, Al-Shibli K, et al. Inverse prognostic impact of angiogenic marker expression in tumor cells versus stromal cells in non-small cell lung cancer. *Clin Cancer Res*. 2007;13:6649-6657. doi:10.1158/1078-0432.CCR-07-0414
- Chatterjee S, Heukamp LC, Siobal M, et al. Tumor VEGF: VEGFR2 autocrine feed-forward loop triggers angiogenesis in lung cancer. *J Clin Invest*. 2013;123:1732-1740. doi:10.1172/JCI65385
- Giatromanolaki A, Koukourakis MI, et al. Activated VEGFR2/KDR pathway in tumor cells and tumor associated vessels of colorectal cancer. *Eur J Clin Invest*. 2007;37:878-886. doi:10.1111/j.1365-2362.2007.01866.x
- Holzer TR, Fulford AD, Nedderman DM, et al. Tumor cell expression of vascular endothelial growth factor receptor 2 is an adverse prognostic factor in patients with squamous cell carcinoma of the lung. *PLoS One*. 2013;8:e80292. doi:10.1371/journal.pone.0080292
- Stitzlein L, Rao P, Dudley R. Emerging oral VEGF inhibitors for the treatment of renal cell carcinoma. *Expert Opin Investig Drugs*. 2019;28:121-130. doi:10.1080/13543784.2019.1559296
- Lopez A, Harada K, Vasilakopoulou M, Shanbhag N, Ajani JA. Targeting angiogenesis in colorectal carcinoma. *Drugs*. 2019;79:63-74. doi:10.1007/s40265-018-1037-9
- Javle M, Smyth EC, Chau I. Ramucirumab: successfully targeting angiogenesis in gastric cancer. *Clin Cancer Res*. 2014;20:5875-5881. doi:10.1158/1078-0432.CCR-14-1071
- Alshangiti A, Chandhoke G, Ellis PM. Anti-angiogenic therapies in non-small-cell lung cancer. *Curr Oncol*. 2018;25:S45-S58. doi:10.3747/co.25.3747
- Paz K, Zhu Z. Development of angiogenesis inhibitors to vascular endothelial growth factor receptor 2. Current status and future perspective. *Front Biosci*. 2005;10:1415-1439. doi:10.2741/1629
- Lee SH. TTAC-0001 (TTAC-0001): a fully human monoclonal antibody targets vascular endothelial growth factor receptor 2 (VEGFR-2). *Arch Pharm Res*. 2011;34:1223-1226. doi:10.1007/s12272-011-0821-9
- Spratlin JL. Ramucirumab (IMC-1121B): monoclonal antibody inhibition of vascular endothelial growth factor receptor-2. *Curr Oncol Rep*. 2011;13:97-102. doi:10.1007/s11912-010-0149-5
- Spratlin JL, Mulder KE, Mackey JR. Ramucirumab (IMC-1121B): a novel attack on angiogenesis. *Future Oncol*. 2010;6:1085-1094. doi:10.2217/fon.10.75
- Spratlin JL, Cohen RB, Eadens M, et al. Phase I pharmacologic and biologic study of ramucirumab (IMC-1121B), a fully human immunoglobulin G1 monoclonal antibody targeting the vascular endothelial growth factor receptor-2. *J Clin Oncol*. 2010;28:780-787. doi:10.1200/JCO.2009.23.7537
- Lu RM, Chiu CY, Liu IJ, Chang YL, Liu YJ, Wu HC. Novel human Ab against vascular endothelial growth factor receptor 2 shows therapeutic potential for leukemia and prostate cancer. *Cancer Sci*. 2019;110:3773-3787. doi:10.1111/cas.14208
- Witte L. Monoclonal antibodies targeting the VEGF receptor-2 (Flk1/KDR) as an anti-angiogenic therapeutic strategy. *Cancer Metastasis Rev*. 1998;17:155-161. doi:10.1023/A:1006094117427
- Shalaby J, Rossant J, Yamaguchi TP, et al. Failure of blood-island formation and vasculogenesis in Flk-1-deficient mice. *Nature*. 1995;376:62-66. doi:10.1038/376062a0
- Hooper AT, Butler JM, Nolan DJ, et al. Engraftment and reconstitution of hematopoiesis is dependent on VEGFR2-mediated regeneration of sinusoidal endothelial cells. *Cell Stem Cell*. 2009;4:263-274. doi:10.1016/j.stem.2009.01.006
- Lu D, Jimenez X, Zhang HF, Bohlen P, Witte L, Zhu ZP. Selection of high affinity human neutralizing antibodies to VEGFR2 from a large antibody phage display library for antiangiogenesis therapy. *Int J Cancer*. 2002;97:393-399. doi:10.1002/ijc.1634
- Holmes K, Roberts OL, Thomas AM, Cross MJ. Vascular endothelial growth factor receptor-2: structure, function, intracellular signaling and therapeutic inhibition. *Cell Signal*. 2007;19:2003-2012. doi:10.1016/j.cellsig.2007.05.013
- Brozzo MS, Bjelic S, Kisko K, et al. Thermodynamic and structural description of allosterically regulated VEGFR-2 dimerization. *Blood*. 2012;119:1781-1788. doi:10.1182/blood-2011-11-390922
- Franklin M, Navarro E, Wang YJ, et al. The structural basis for the function of two anti-VEGF receptor 2 antibodies. *Structure*. 2011;19:1097-1107. doi:10.1016/j.str.2011.01.019
- Hlatky L, Hahnfeldt P, Folkman J. Clinical application of antiangiogenic therapy: microvessel density, what it does and doesn't tell us. *J Natl Cancer Inst*. 2002;94:883-893. doi:10.1093/jnci/94.12.883
- Kapoor S, Shenoy SP, Bose B. CD34 cells in somatic, regenerative and cancer stem cells: developmental biology, cell therapy, and omics big data perspective. *J Cell Biochem*. 2020;121:3058-3069. doi:10.1002/jcb.29571
- Folkman J. Tumor angiogenesis: therapeutic implications. *N Engl J Med*. 1971;285:1182-1186. doi:10.1056/NEJM197111182852108
- Nasir A. *Angiogenic Signaling Pathways and Anti-Angiogenic Therapies in Human Cancer: Applications in Precision Medicine*. Springer International Publishing; 2019.
- Ferrara N, Kerbel RS. Angiogenesis as a therapeutic target. *Nature*. 2005;438:967-974. doi:10.1038/nature04483
- Dev IK, Dornsife RE, Hopper TM, et al. Antitumor efficacy of VEGFR2 tyrosine kinase inhibitor correlates with expression of VEGF and its receptor VEGFR2 in tumor models. *Br J Cancer*. 2004;91:1391-1398. doi:10.1038/sj.bjc.6602109

38. Zhu Z, Hattori K, Zhang H, et al. Inhibition of human leukemia in an animal model with human antibodies directed against vascular endothelial growth factor receptor 2. Correlation between antibody affinity and biological activity. *Leukemia*. 2003;17:604-611.
39. Shi L, Lehto SG, Zhu DX, et al. Pharmacologic characterization of AMG 334, a potent and selective human monoclonal antibody against the calcitonin gene-related peptide receptor. *J Pharmacol Exp Ther*. 2015;356:223-231. doi:10.1124/jpet.115.227793
40. Carmeliet P, Jain RK. Molecular mechanisms and clinical applications of angiogenesis. *Nature*. 2011;473:298-307. doi:10.1038/nature10144
41. Danial NN, Korsmeyer SJ. Cell death: critical control points. *Cell*. 2004;116:205-219. doi:10.1016/S0092-8674(04)00046-7
42. Yuan J, Yankner BA. Apoptosis in the nervous system. *Nature*. 2000;407:802-809.
43. Alladina SJ, Song JH, Davidge ST, Hao C, Easton AS. TRAIL-induced apoptosis in human vascular endothelium is regulated by phosphatidylinositol 3-kinase/Akt through the short form of cellular FLIP and Bcl-2. *J Vasc Res*. 2005;42:337-347. doi:10.1159/000086599
44. Li P, Zhou LB, Zhao T, et al. Caspase-9: structure, mechanisms and clinical application. *Oncotarget*. 2017;8:23996-24008. doi:10.18632/oncotarget.15098
45. Giatromanolaki A, Koukourakis MI, Turley H, Sivridis E, Harris AL, Gatter KC. Phosphorylated KDR expression in endometrial cancer cells relates to HIF1 α /VEGF pathway and unfavorable prognosis. *Mod Pathol*. 2006;19:701-707. doi:10.1038/modpathol.3800579
46. Yoh K, Hosomi Y, Kasahara K, et al. A randomized, double-blind, phase II study of ramucirumab plus docetaxel vs placebo plus docetaxel in Japanese patients with stage IV non-small cell lung cancer after disease progression on platinum-based therapy. *Lung Cancer*. 2016;99:186-193. doi:10.1016/j.lungcan.2016.07.019

SUPPORTING INFORMATION

Additional supporting information can be found online in the Supporting Information section at the end of this article.

How to cite this article: Cao Y, Sun C, Huo G, et al. Novel hKDR mouse model depicts the antiangiogenesis and apoptosis-promoting effects of neutralizing antibodies targeting vascular endothelial growth factor receptor 2. *Cancer Sci*. 2023;114:115-128. doi: [10.1111/cas.15594](https://doi.org/10.1111/cas.15594)